Spin-label EPR on Disordered and Amyloid Proteins

Hashemi Shabestari, M.

CHAPTER 7

STRUCTURE AND FIRST EPR CHARACTERIZATION OF HELICAL PEPTIDES WITH TOAC SPIN LABELS: MODELS FOR SHORT DISTANCES

For structure determination in biophysical systems electron paramagnetic resonance (EPR) is rapidly gaining ground. Proteins labeled specifically with two nitroxide spin labels can be prepared, and several EPR methods are available for distance determination, which makes it possible to determine distance constraints. However, such methods require frozen solutions, potentially causing non-physiological states of the sample. Here we target spin-spin interaction in liquid solution at room temperature using rigid model compounds. A series of helical peptides is synthesized with pairs of spin labels separated by three, four, and five amino acids. To avoid flexibility, the non-coded nitroxyl containing α-amino acid TOAC that is rigidly connected with the peptide backbone is used. The EPR spectra of the peptides show a decreasing amount of coupling between the two spin labels within this series, which provides a first characterization of these models.

Maryam Hashemi Shabestari, Martin van Son, Alessandro Moretto, Marco Crisma, Claudio Toniolo, Martina Huber.

7.1 Introduction

Biological systems are preferably studied in liquid solution at room temperature because freezing a peptide or a protein can change or even destroy the three-dimensional structure of interest. Most EPR methods for distance determination require freezing the sample [1-6]. To address this problem, in the present work we investigate spin-spin interactions in model peptide systems in liquid solution. Such peptides have to be rigid to serve as useful model compounds. More specifically, we analyze a series of peptides consisting of stretches of the non-coded, host α-amino acid α-aminoisobutyric acid (Aib), combined with one or two 4-amino-1-oxyl-2,2,6,6-tetramethylpiperidine-4-carboxylic acid (TOAC) guest residues. Both TOAC [7-13] and Aib [14-16] are known to stabilize regular 3_{10}-helices [14,16-19]. The backbone and side-chain conformations of TOAC are remarkably constrained, providing well-defined distances between the stable nitroxide free radicals of two TOAC residues. Flexibility, as resulting from the commonly used spin labels linked to the cysteine side chain in proteins, is thus avoided. Our series comprises a full set of peptides, from two to five intervening Aib residues, with incrementally increased TOAC…TOAC separations. The following compounds were investigated:

(i)	Z-$(Aib)_9$-OMe	NONA	unlabeled
(ii)	Z-$(Aib)_5$-TOAC-Aib-OMe	$HEPTA_6$	monoradical
(iii)	Z-$(Aib)_6$-TOAC-Aib-OMe	$OCTA_7$	monoradical
(iv)	Fmoc-Aib-TOAC-$(Aib)_7$-OMe	$NONA_2$	monoradical
(v)	Fmoc-$(Aib)_2$-TOAC-$(Aib)_2$-TOAC-Aib-OMe	$HEPTA_{3,6}$	biradical
(vi)	Fmoc-TOAC-$(Aib)_3$-TOAC-Aib-OMe	$HEXA_{1,5}$	biradical
(vii)	Fmoc-Aib-TOAC-$(Aib)_4$-TOAC-Aib-OMe	$OCTA_{2,7}$	biradical
(viii)	Fmoc-Aib-TOAC-$(Aib)_5$-TOAC-Aib-OMe	$NONA_{2,8}$	biradical

Here Z is benzyloxycarbonyl, OMe is methoxy, and Fmoc is fluorenyl-9-methyloxycarbonyl. We address the sub-nanometer distances between two TOAC residues in the biradical peptides and compare them with a set of monoradical peptides that are matched in size. We determine the exchange interaction, J, in liquid solution using continuous-wave (cw) EPR. For selected peptides also the dipolar interaction in frozen solution was studied.

In the sub-nanometer distance regime in liquid solution, the spin-spin interaction should manifest itself primarily as the exchange interaction, J. In the weak-exchange limit, the spectra appear as those of the isolated radicals. For nitroxides

characteristic three-line spectra result, which come from the isotropic hyperfine interaction A_N of the electron spin with the ^{14}N, I = 1 nucleus. A strong-exchange interaction ($J \gg A_N$) results in a five-line spectrum. The magnitude of J is related to the orbital overlap, and often J is believed to decay exponentially with distance [20]. Orbital overlap through the bonds, which are linking the centers of spin density can also promote exchange interaction.

For selected peptides the dipolar interaction was studied in frozen solution with X-band (9.5 GHz) and W-band (95 GHz) EPR. At W-band, the spectral resolution increases and the information on magnetic parameters and molecular orientations, which is hidden under the broad lines in spectra that are obtained at X-band can be extracted. Furthermore, the higher resolution at W-band enables the detection of smaller dipolar interactions, i.e., longer distances than in X-band. Also, relative orientations of spin labels are accessible [21].

The rigid biradical peptides investigated enable a systematic study of the exchange interaction. Overall, a decrease of J with increasing separation of the two TOAC residues is observed. We speculate that J is dominated by through-bond rather than through-space interaction. Careful line-shape analysis gives insight into the intra-radical interactions.

7.2 Materials and methods

7.2.1 Synthesis and characterization of peptides

Peptides NONA [7], $NONA_2$ (labeled as $NONA_9$ in [7]) $NONA_{2,8}$ [7], and $HEPTA_{3,6}$ [22], have already been described. The difficult syntheses of the other very highly constrained TOAC/Aib peptides mentioned in this paper have been performed in solution [23] either: step-by-step by using the 1-(3-dimetylamino)propyl-3-ethyl-carbodiimide/7-aza-1-hydroxy-1,2,3-benzotriazole method [24] ($HEXA_5$, $HEXA_{1,5}$, and $OCTA_{2,7}$) or by the segment condensation procedure using the isolated and uncharacterized intermediate 5(4*H*)-oxazolones from Z-$(Aib)_3$-OH [25] and Z-$(Aib)_5$-OH [25] for $HEPTA_6$ and $OCTA_7$, respectively. The chromatographically pure peptides show the following physical and analytical data: (a) $HEPTA_6$: melting point 219-221° C (from EtOAc – PE); infrared (IR) (KBr) 3322, 1712, 1664 cm^{-1}. (b) $OCTA_7$: melting point 222-224° C (from EtOAc – PE); IR (KBr) 3318, 1712, 1662 cm^{-1}. (c) $HEXA_{1,5}$: melting point 146-147° C (from EtOAc – PE); IR (KBr) 3331, 1669 cm^{-1}. (d) $OCTA_{2,7}$: melting point 160-162°C (from EtOAc – PE); IR (KBr) 3306, 1659 cm^{-1}.

7.2.2 Fourier transform infrared absorption spectroscopy

Fourier transform infra red absorption spectra were recorded using a Perkin-Elmer 1720 X FT-IR spectrophotometer, nitrogen-flushed, with a sample shuttle device and at 2 cm^{-1} nominal resolution, averaging 100 scans. Solvent (baseline) spectra were recorded under the same conditions. Cells with CaF_2 windows and path lengths of 0.1 and 1.0 mm were used. Spectrograde deuterochloroform (99.8 % deuterated) was obtained from Fluka.

7.2.3 EPR spectroscopy

The X-band cw EPR measurements were performed both at room temperature (293 K) and at 80 K using an Elexsys 680 (Bruker BioSpin GmbH, Rheinstetten, Germany) spectrometer equipped with a rectangular cavity. For the room temperature measurements microwave power, modulation frequency, and modulation amplitude were 0.3994 mW, 100 kHz, and 30 μT, respectively, and accumulation time was about 20 minutes per spectrum. In the frozen solution at X-band microwave power, modulation frequency, and modulation amplitude were 0.159 mW, 100 kHz, and 0.2 mT, respectively.
For room temperature W-band measurements, a modulation frequency of 100 kHz and a modulation amplitude of 0.1 mT were applied. The standard 95 MHz sample clamp was used with the usual sample holder to place the sample properly in the resonator. For the frozen solution W-band measurements, microwave power, modulation frequency, and modulation amplitude were 5.0 $*10^{-5}$ mW, 100 kHz, and 0.5 mT, respectively.

7.2.4 Preparation of the samples

All peptides were dissolved in acetonitrile (Biotech. grade, ≥ 99.93 %, Sigma-Aldrich). For room temperature X-band measurements, all the peptide samples were degassed and prepared in quartz tubes with an outer diameter of 4 mm and an inner diameter of 1.5 mm. The samples were then subjected to seven freeze-pump-thaw cycles. To freeze the sample, liquid nitrogen was used. The sample was thawed to room temperature. While the samples were frozen, the quartz tubes were connected to a rotary vacuum pump for 5 minutes and disconnected from the pump before thawing the sample. Finally the degassed samples were flame-sealed. The room temperature W-band samples were prepared in suprasil quartz capillaries, with an inner diameter of 0.125 mm and an outer diameter of 0.25 mm, from Wilmad-Lab glass (Buena, NJ, USA). The capillaries were sealed at one end. A Wilmad suprasil quartz tube with an inner diameter of 0.60 mm and an outer diameter of 0.84 mm,

which was sealed at one end, was used as an outside tube. The concentration of the TOAC spin label in all liquid solution samples was 0.1 mM.

For the measurements in frozen solution at X-band, samples were prepared in quartz tubes with an outer diameter of 4 mm and were frozen in liquid nitrogen before inserting them in the pre-cooled helium gas-flow cryostat. For 80 K W-band measurements, the samples were measured in Wilmad suprasil quartz tubes with an inner diameter of 0.60 mm and an outer diameter of 0.84 mm that were sealed at one end. Both the monoradical, $NONA_2$, and the biradical, $NONA_{2,8}$, samples were diluted with NONA, the Aib peptide at a 1 to 10 diamagnetically dilution. The concentration of $NONA_2$ and $NONA_{2,8}$ in frozen solution was 0.2 mM and 0.1 mM, respectively.

7.2.5 Simulation

The spectra were simulated using Matlab and the EasySpin package [26]. For the simulation the following parameters were used: g = [2.009, 2.006, 2.003] [7], A_{xx} = A_{yy} = 0.553, and A_{zz} = 3.375 mT. The three-line spectra were simulated using a Gaussian line-shape. The five-line spectra were simulated using an equal-amount contribution of a Gaussian and a Lorentzian line-shape [26].

For the biradical peptides, the treatment of the effect of J depends on the type of spectrum. For compounds with a three-line spectrum, the spectra were simulated with the chili subroutine of EasySpin as an S = ½ system. For the five-line spectra, the effect of the exchange interaction was included explicitly in the simulation using the pepper subroutine as two coupled S = ½ systems. The presence of a sharp three-line component in the five-line spectrum was taken into account in the simulation by adding a mono-radical contribution to each spectrum using the chili subroutine. We checked the presence of satellite lines for $HEXA_{1,5}$ and $OCTA_{2,7}$ by measuring at higher powers, larger sweep widths and higher concentrations (about 5 mM, non degassed). We also increased the modulation amplitude. However, no satellite lines were detected.

7.3 Results

7.3.1 Conformational analysis

We carried out a conformational analysis of all TOAC-labeled $(Aib)_n$ host peptides (from hexamers to nonamers) studied in this work in $CDCl_3$, a secondary-structure supporting solvent. Since neither circular dichroism (because all peptides are achiral) nor nuclear magnetic resonance (because all peptides contain at least one stable paramagnetic free radical) are appropriate spectroscopies with these compounds, we relied heavily on FT-IR absorption. The N-H stretching (amide A)

spectral region proved to be the most conformationally informative. Here, all peptides are characterized by two bands: a much weaker one, seen at 3435-3418 cm^{-1} (free, solvated NH groups) and a much more intense one at 3339-3318 cm^{-1} (H-bonded NH groups) [15,27,28]. With increasing main-chain length, the stronger band moves to lower wave numbers and increases in intensity [15]. The role of peptide concentration, at least below 5×10^{-3} M, is of minor significance, which indicates that the observed C=O…H-N H-bonds are mostly intra-molecular. The ratios of the integrated molar extinction coefficients of the H-bonded versus free NH groups point clearly to almost fully developed 3_{10}-helical [14,16-19] peptide structures [15]. These findings are not unexpected on the basis of literature data of medium-sized peptides rich in the known helicogenic TOAC [8,13] and Aib [14-16] residues in $CDCl_3$ solution and in the crystal state.

7.3.2 Room temperature cw EPR

Figure 7.1 presents the room temperature spectra of the monoradical and the biradical peptides. The spectra of the monoradical peptides consist of three narrow lines. The spectra of the biradical peptides can be grouped into two distinct classes: the $HEPTA_{3,6}$ and the $HEXA_{1,5}$ peptides with a five-line spectrum and the $OCTA_{2,7}$ and the $NONA_{2,8}$ peptides with a three-line spectrum. The five-line spectra have broader lines than those of the monoradical peptides and a contribution of a narrow-line spectrum consisting of three lines marked in figure 7.1.

The two classes of spectra are simulated by different approaches. For the two biradical peptides that have a five-line spectrum, the contribution of exchange interaction is larger than the hyperfine coupling of the ^{14}N nucleus in the TOAC spin label (table 7.1), and we consider the contribution of J explicitly in the simulation. For the $HEPTA_{3,6}$ peptide, the value of J is larger than 900 MHz. For $HEXA_{1,5}$, the next biradical peptide in the series, the value of J is 800 MHz. For the three-line-spectra of the $OCTA_{2,7}$ and $NONA_{2,8}$ peptides, the value of J must be smaller than 9 MHz because for values of J above 9 MHz a significant deviation of the simulation from the observed three-line spectra occurs, a deviation that is not visible in the experimental spectra. Given that small value of J, we do not explicitly consider J in the simulation.

To exactly match the line-shape of the simulated to the experimental spectra for all biradical peptides, additional parameters are needed (figure 7.2 and table 7.1). The spectra of the $HEXA_{1,5}$ and the $HEPTA_{3,6}$ peptides are simulated by two components, one component with a large J-value, representing the biradical, and the other representing a monoradical component. The monoradical contribution is simulated with the parameters of the respective monoradical peptide (table 7.1). The

spectra of the second class of peptides, the $OCTA_{2,7}$ and the $NONA_{2,8}$ peptides are fully described by a single component. The $NONA_{2,8}$ peptide is simulated with an isotropic rotation correlation time, similar to the value we used to simulate the corresponding monoradical, $NONA_2$. The simulated spectrum of the $OCTA_{2,7}$ peptide does not fit as well to the isotropic rotation model as the $NONA_{2,8}$ peptide. The deviation of the simulated low-field line from the experimental one derives either from an anisotropic rotation or from a contribution of J in the order of 9 MHz. The spectrum of the $OCTA_{2,7}$ peptide can be fitted with an anisotropic-rotation model using the best-fit option in the EasySpin program (table 7.1). However, we cannot exclude J-coupling, as it would produce qualitatively similar features. For the $NONA_2$ and the $NONA_{2,8}$ peptides, EPR spectra are also acquired at W-band. The spectra of $NONA_2$ and $NONA_{2,8}$ are identical (figure 7.3), which reveals that for these peptides the EPR spectra at W-band frequencies are dominated by motion, rather than by the spin-spin interaction.

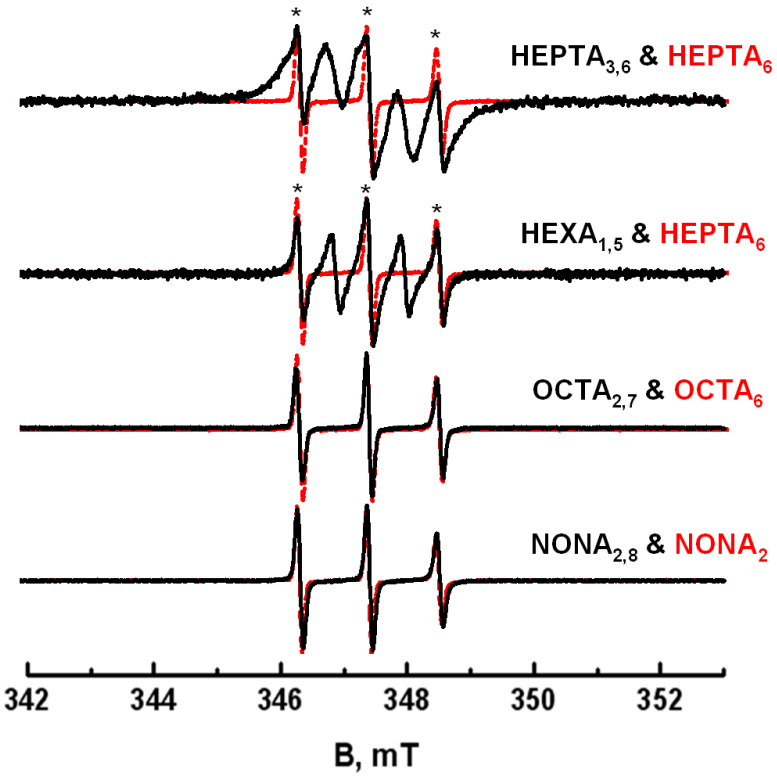

Figure 7.1 The room temperature X-band EPR spectra of monoradical (red) and biradical (black) peptides. Comparison of mono- with biradical peptides are shown from top to bottom: $HEPTA_{3,6}$ with monoradical $HEPTA_6$; $HEXA_{1,5}$ with monoradical $HEPTA_6$; $OCTA_{2,7}$ with monoradical $OCTA_7$, and $NONA_{2,8}$ with monoradical $NONA_2$. The black asterisks indicate the presence of narrow lines on top of the broad lines in the spectrum of the biradical peptides.

Table 7.1 Parameters used for the simulation of the liquid solution X-band ER spectra of the monoradical and biradical peptides. Given on the right are parameters for monoradicals: rotation correlation times τ_r and line-widths. On the left are simulation parameters for biradicals (τ_r, line-widths, and the line-shape: mixture of Gaussian and Lorentzian). The simulation parameters and the relative contribution of monoradical species to these spectra is given on the right. For $HEPTA_{3,6}$ and $HEXA_{1,5}$ the exchange interaction is explicitly considered. For details see text.

peptides		τ_r (ns)	line-width[a] (mT)	
$HEPTA_6$		0.13	0.130	
$OCTA_7$		0.15	0.130	
$NONA_2$		0.17	0.130	

peptides	parameters used for the simulation of biradical peptides					monoradical contribution to biradical spectra		
	Relative position of the 2nd TOAC in the helix	J-coupling (MHz)	τ_r (ns)	line-width (mT)		τ_r (ns)	line-width[a] (mT)	monoradical component in biradical spectra %
				Gaussian	Lorentzian			
$HEPTA_{3,6}$	4	> 900	n.a.[b]	0.450	0.480	0.13	0.130	3
$HEXA_{1,5}$	5	800	n.a.	0.000	0.290	0.13	0.130	23
$OCTA_{2,7}$	6	< 9	0.15[c]	0.098	0.037	n.a.	n.a.	n.a.
$NONA_{2,8}$	7	< 9	0.17	0.110	0.037	n.a.	n.a.	n.a.

[a] Gaussian single-component line
[b] not applicable
[c] The EPR simulation parameters for the $OCTA_{2,7}$ peptide using an anisotropic rotation with axial rotation tensor; Best-fit parameters: $\tau_{\parallel} = 0.016, \tau_{\perp} = 0.78, \tau_{iso} = 0.046$

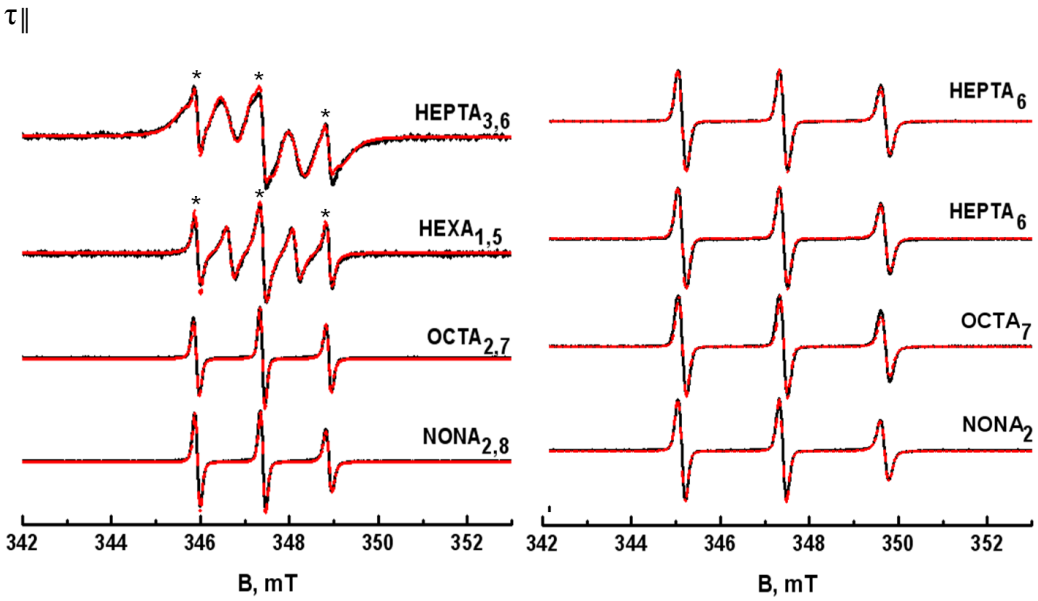

Figure 7.2 The room temperature X-band EPR spectra of monoradical and biradical peptides compared with the simulation. Simulated spectra are shown in red and the experimental ones are shown in black. On the left, the spectra of $HEPTA_{3,6}$, $HEXA_{1,5}$, $OCTA_{2,7}$, and $NONA_{2,8}$ are shown. On the right, the spectra of $HEPTA_6$, $OCTA_7$, and $NONA_2$ are shown. The black asterisks indicate the presence of narrow lines (monoradical contribution) on top of the broad lines in the spectrum of the biradical peptides.

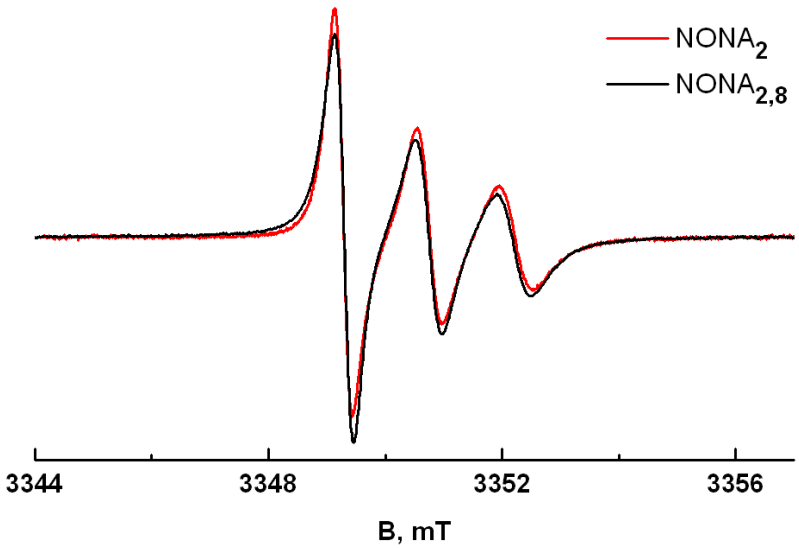

Figure 7.3 The room temperature W-band EPR spectra of the $NONA_2$ peptide (red) and the $NONA_{2,8}$ peptide (black). The spectra of $NONA_2$ and $NONA_{2,8}$ are similar. The spectra are normalized to the number of spins in each sample.

7.3.3 $NONA_2$ and $NONA_{2,8}$ at X-band, in frozen solution

In frozen solution, in addition to the exchange interaction, the dipolar interaction can be determined. However, the peptides seem to aggregate in frozen solution, as evidenced by the line broadening of $NONA_2$ relative to a reference sample containing the MTS spin label, which is prepared in the same solvent and measured under the same conditions (figure 7.4).

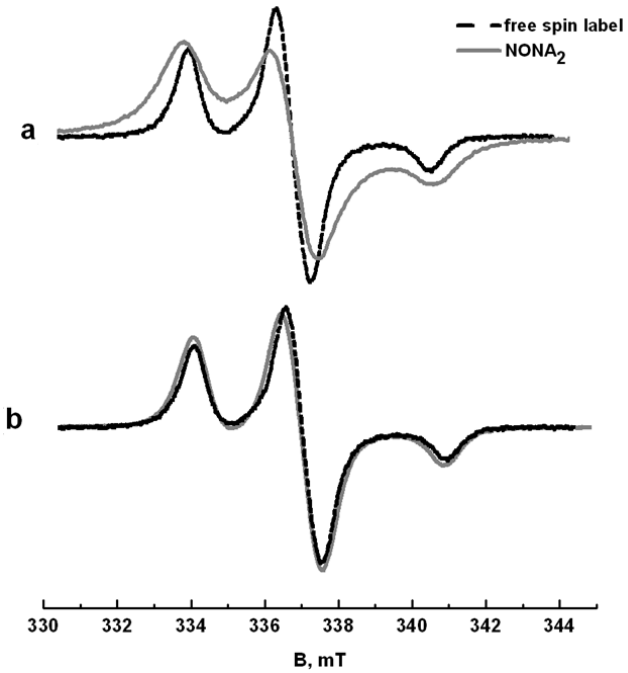

Figure 7.4 Frozen solution X-band EPR spectra of the $NONA_2$ peptide and the free MTS spin label in the same solvent. a: Pure $NONA_2$ peptide (grey line) and free MTS spin label (black line). b: Diamagnetically diluted (1:10) $NONA_2$ peptide (grey line) and free MTS spin label (black line). In a the lines of the $NONA_2$ peptide are broader compared to the lines in b, owing to the intermolecular spin-spin interaction. The spectra are normalized to the number of spins in each sample.

To suppress intermolecular spin-spin interaction, diamagnetic dilution with the Aib-only peptide NONA is applied [29]. We investigated 1:5 and 1:10 ratios of $NONA_2$ to NONA. At both ratios the spectra have the same line-width as the reference sample has. Therefore, the biradical $NONA_{2,8}$ was investigated at a 1 to 10 diamagnetic dilution. For $NONA_{2,8}$ compared with $NONA_2$, the lines are broader, which results from the dipolar interaction in the $NONA_{2,8}$ peptide (figure 7.5).

Distances derived from the second-moment analysis [30] of the $NONA_2$ and the $NONA_{2,8}$ spectra result in a distance of 1.1 nm, which is in good agreement with the distance of 1.2 nm reported from the X-ray structure [7].

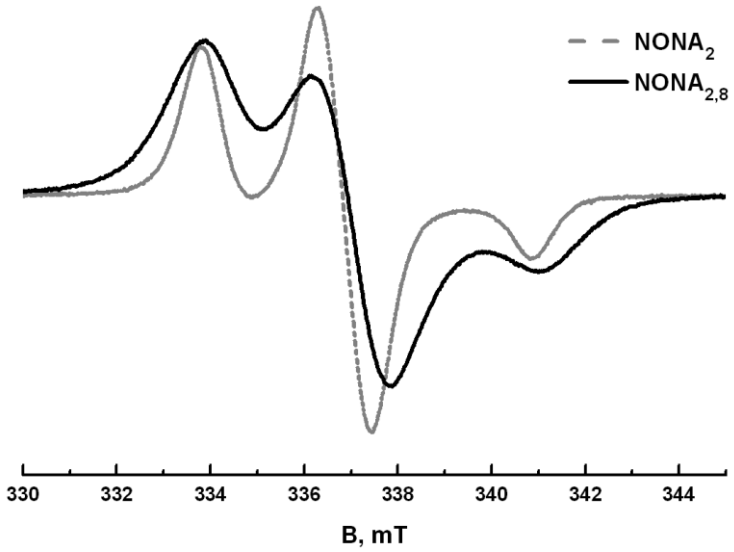

Figure 7.5 Frozen solution X-band EPR spectra of the $NONA_2$ peptide (grey line) and the $NONA_{2,8}$ peptide (black line). Both peptides are diamagnetically diluted (1:10). The lines of the $NONA_2$ peptide are narrower compared to those of the $NONA_{2,8}$ peptide. The spectra are normalized to the number of spins in each sample.

7.3.4 $NONA_2$ and $NONA_{2,8}$ at W-band, in frozen solution

The EPR spectra of both $NONA_2$ and $NONA_{2,8}$ at W-band (figure 7.6) are acquired from the same diamagnetically diluted samples as used for X-band in frozen solution (1 to 10).

At W-band, the g-tensor resolution increases, making it possible to resolve the rhombic g-tensor, while at X-band the nitroxide spectrum is dominated by the hyperfine interaction with the nitrogen nucleus. Similar to the result at X-band, the lines of $NONA_{2,8}$ are broadened with respect to $NONA_2$. The higher resolution at W-band was used by Carlotto et al. [33] to determine the distance and relative orientation of the TOAC radicals in $NONA_{2,8}$.

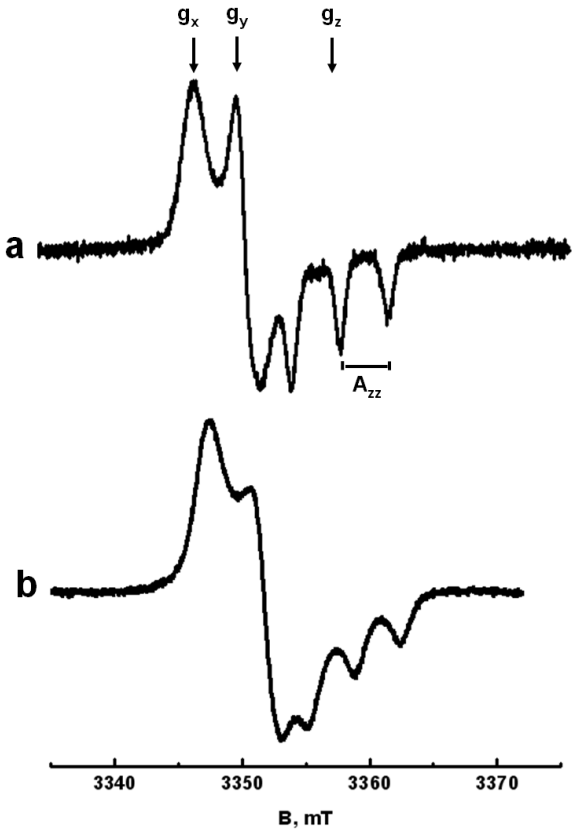

Figure 7.6 Frozen solution W-band EPR spectra of a: the $NONA_2$ peptide and b: the $NONA_{2,8}$ peptide. The position of the spectral features at g_x, g_y, g_z, and the hyperfine splitting A_{zz} are indicated.

7.4 Discussion

We have investigated a set of biradical peptides built from the non-natural amino-acid Aib, both in liquid and in frozen solution. In liquid solution at room temperature, the peptides have spectra that are in the motionally narrowed regime. The spectra of the biradicals are determined primarily by the exchange interaction [32]. In the strong-exchange regime, where $J \gg A_N$, the EPR spectrum is characterized by a five-line pattern with intensities 1:2:3:2:1, while in the weak-exchange regime the EPR spectrum has three lines of equal intensity. The spectra of biradicals $HEPTA_{3,6}$ and $HEXA_{1,5}$ are in the strong-exchange regime. The difference in the line-shapes between $HEPTA_{3,6}$ and $HEXA_{1,5}$ suggests a larger J for $HEPTA_{3,6}$ or an additional dynamic process. The biradicals $OCTA_{2,7}$ and $NONA_{2,8}$ are in the weak-exchange limit. Because the effect of J on the spectrum is minimal and because no

simulation program combines J-interaction with restricted mobility we have simulated the spectra of the $OCTA_{2,7}$ and the $NONA_{2,8}$ peptides as two independent spins. Therefore, only upper limits of J can be determined. The spectrum of $OCTA_{2,7}$ shows deviations from the isotropic-motion regime. Whether this deviation reflects anisotropic motion or a J-value that is slightly larger than 9 MHz is not clear yet. The main result is that the J-coupling decreases with increasing residue separation in the sequence.

7.4.1 Origin of the narrow-line contribution

The presence of a sharp narrow-line component is prominent in the five-line-spectrum of the $HEPTA_{3,6}$ and $HEXA_{1,5}$ peptides. There are two possibilities for the origin of this component. First, the sharp component may arise from a minimally populated conformation of the peptides, which leads to increased separation between the labels such that we have a contribution of a low J-value in addition to the dominant high J-value conformation of the peptide. A second possibility is that in a fraction of the peptides one of the nitroxides is chemically degraded. The rigidity of the peptides investigated argues against the presence of minority conformations in which J is small. Therefore we attribute the narrow-line component to a monoradical contamination.

7.4.2 The relation between structure and J-coupling

The strength of the exchange interaction is often considered to decay exponentially with distance and has been used to obtain a qualitative ranking of the distance of spin-label positions [32]. For the set of peptides that are investigated here, the separation between the TOAC residues increases by one residue each in the series.
The distance between the nitroxide groups, i.e., the through-space distance does not increase through the series (table 7.2). For example, the distance between residues one and five (in $HEXA_{1,5}$) is similar to the distance between two and eight (in $NONA_{2,8}$). So if J would scale with the distance between the nitroxide groups through space, the $HEXA_{1,5}$ and $NONA_{2,8}$ peptides should have similar values of J. However, the $NONA_{2,8}$ peptide has a very small J, while the $HEXA_{1,5}$ has a much larger J, a clear indication that the through-space distance of the nitroxides does not dominate J. The number of bonds between the nitroxides does increase monotonically within the series from $HEXA_{1,5}$ to $NONA_{2,8}$. Particularly, the number of bonds between the nitroxides in $HEXA_{1,5}$ is smaller than those in the $NONA_{2,8}$ peptide, nicely following the trend in J. The difference between these two peptides shows that the through-bond contribution to J plays a major role.

Table 7.2 Comparison of the biradical peptides investigated. The number of covalent bonds between the two TOAC spin labels in each biradical peptide and the distance between the mid-points of the N-O bonds of the two TOAC labels in the 3_{10}-helix are given.

peptide	position of the two TOAC labels	distance between the two TOAC residues (Å)	number of covalent bonds	J-coupling (MHz)
HEPTA$_{3,6}$	i, i + 3	6.5[a]	15	> 900
HEXA$_{1,5}$	i, i + 4	11.6[b]	18	800
OCTA$_{2,7}$	i, i + 5	14.6[b]	21	< 9
NONA$_{2,8}$	i, i + 6	12.6[c]	24	< 9

[a] Experimentally determined i, i + 3 distance from the X-ray diffraction structure of HEPTA$_{3,6}$ [33].
[b] Calculated from a 3_{10}-helical peptide model.
[c] Experimentally determined i, i + 6 distance from the X-ray diffraction structure of OCTA$_{1,4,7}$ [34].

7.4.3 The contribution of dipolar interaction

In the spectra in liquid solution no dipolar interaction is observed, although this interaction is expected to be large in view of the distance between the TOAC residues. The absence of dipolar broadening in the spectra proves that the rotation of the peptides is fast enough to average the dipolar interaction.
In frozen solution, both the exchange and dipolar interactions are detectable. However, in frozen solution these peptides tend to aggregate and intermolecular interactions interfere with the intra-molecular interactions. To avoid this interference, we applied diamagnetic dilution. Comparison of the diluted monoradical vs. biradical peptides provides us with intra-molecular information, i.e., the spin-spin distance in a biradical peptide. The value of 1.1 nm obtained from the line-shape analysis agrees with the results from X-ray crystallography [7].

7.4.4 Summary and conclusions

The series of biradical peptides enabled a systematic study of the exchange interaction. We demonstrate that in these helical peptides the through-bond contribution dominates over the through-space contribution, which gives rise to a substantial J even over a separation of 12 Å. We are pursuing these studies with the quantum-chemical approach applied in reference [7], which will give insight into the electronic structure of these peptides.

Reference List

[1] W. L. Hubbell, C. Altenbach, *Current Opinion in Structural Biology* **1994,** *4* 566-573.
[2] Q. Cai, A. K. Kusnetzow, W. L. Hubbell, I. S. Haworth, G. P. Gacho, E. N. Van, K. Hideg, E. J. Chambers, P. Z. Qin, *Nucleic Acids Res.* **2006,** *34* 4722-4730.
[3] G. Jeschke, *Chemphyschem* **2002,** *3* 927-932.
[4] G. Jeschke, A. Bender, H. Paulsen, H. Zimmermann, A. Godt, *J.Magn Reson.* **2004,** *169* 1-12.
[5] G. Jeschke, H. Zimmermann, A. Godt, *J.Magn Reson.* **2006,** *180* 137-146.
[6] G. Jeschke, Y. Polyhach, *Phys.Chem.Chem.Phys.* **2007,** *9* 1895-1910.
[7] S. Carlotto, M. Zerbetto, M. H. Shabestari, A. Moretto, F. Formaggio, M. Crisma, C. Toniolo, M. Huber, A. Polimeno, *J.Phys.Chem.B* **2011,** *115* 13026-13036.
[8] M. Crisma, J. R. Deschamps, C. George, J. L. Flippen-Anderson, B. Kaptein, Q. B. Broxterman, A. Moretto, S. Oancea, M. Jost, F. Formaggio, C. Toniolo, *J.Pept.Res.* **2005,** *65* 564-579.
[9] M. Grimaldi, M. Scrima, C. Esposito, G. Vitiello, A. Ramunno, V. Limongelli, G. D'Errico, E. Novellino, A. M. D'Ursi, *Biochim.Biophys.Acta* **2010,** *1798* 660-671.
[10] P. Hanson, G. Martinez, G. Millhauser, F. Formaggio, M. Crisma, C. Toniolo, C. Vita, *Journal of the American Chemical Society* **1996,** *118* 271-272.
[11] V. Monaco, F. Formaggio, M. Crisma, C. Toniolo, P. Hanson, G. L. Millhauser, *Biopolymers* **1999,** *50* 239-253.
[12] S. Stoller, G. Sicoli, T. Y. Baranova, M. Bennati, U. Diederichsen, *Angew.Chem.Int.Ed Engl.* **2011,** *50* 9743-9746.
[13] C. Toniolo, M. Crisma, F. Formaggio, *Biopolymers* **1998,** *47* 153-158.
[14] I. L. Karle, P. Balaram, *Biochemistry* **1990,** *29* 6747-6756.
[15] C. Toniolo, G. M. Bonora, V. Barone, A. Bavoso, E. Benedetti, B. Diblasio, P. Grimaldi, F. Lelj, V. Pavone, C. Pedone, *Macromolecules* **1985,** *18* 895-902.
[16] C. Toniolo, M. Crisma, F. Formaggio, C. Peggion, *Biopolymers* **2001,** *60* 396-419.
[17] E. Benedetti, B. B. Di, V. Pavone, C. Pedone, C. Toniolo, M. Crisma, *Biopolymers* **1992,** *32* 453-456.
[18] K. A. Bolin, G. L. Millhauser, *Accounts of Chemical Research* **1999,** *32* 1027-1033.
[19] C. Toniolo, E. Benedetti, *Trends Biochem.Sci.* **1991,** *16* 350-353.
[20] Luckhurst G.R., in *spin labeling***1976**, p. pp. 133-179.
[21] E. J. Hustedt, A. I. Smirnov, C. F. Laub, C. E. Cobb, A. H. Beth, *Biophys.J.* **1997,** *72* 1861-1877.
[22] M. Zerbetto, S. Carlotto, A. Polimeno, C. Corvaja, L. Franco, C. Toniolo, F. Formaggio, V. Barone, P. Cimino, *Journal of Physical Chemistry B* **2007,** *111* 2668-2674.
[23] Goodman M., A. Felix, C. Moroder, C. Toniolo, Ed.: G. Thieme: Stuttgart)**20103**, p. pp. 292-310.
[24] L. A. Carpino, *Journal of the American Chemical Society* **1993,** *115* 4397-4398.
[25] D. S. Jones, *Proceedings of the Cambridge Philosophical Society-Mathematical and Physical Sciences* **1965,** *61* 223-&.
[26] S. Stoll, A. Schweiger, *Journal of Magnetic Resonance* **2006,** *178* 42-55.
[27] M. H. Baron, C. Deloze, C. Toniolo, G. D. Fasman, *Biopolymers* **1978,** *17* 2225-2239.
[28] G. M. Bonora, C. Mapelli, C. Toniolo, R. R. Wilkening, E. S. Stevens, *International Journal of Biological Macromolecules* **1984,** *6* 179-188.
[29] F. Scarpelli, M. Drescher, T. Rutters-Meijneke, A. Holt, D. T. Rijkers, J. A. Killian, M. Huber, *J.Phys.Chem.B* **2009,** *113* 12257-12264.
[30] H. J. Steinhoff, *Frontiers in Bioscience* **2002,** *7* C97-C110.
[31] J. C. McNulty, J. L. Silapie, M. Carnevali, C. T. Farrar, R. G. Griffin, F. Formaggio, M. Crisma, C. Toniolo, G. L. Milhauser, *Biopolymers* **2000,** *55* 479-485.
[32] C. J. Gorter, J. H. van Vleck, *Physical Review* **1947,** *72* 1128-1129.
[33] S. Carlotto, P. Cimino, M. Zerbetto, L. Franco, C. Corvaja, M. Crisma, F. Formaggio, C. Toniolo, A. Polimeno, V. Barone, *J.Am.Chem.Soc.* **2007,** *129* 11248-11258.
[34] E. Sartori, C. Corvaja, S. Oancea, F. Formaggio, M. Crisma, C. Toniolo, *Chemphyschem* **2005,** *6* 1472-1475.